

# The Surprising Effectiveness of Multimodal Large Language Models for Video Moment Retrieval

Boris Meinardus<sup>1,2</sup>, Anil Batra<sup>3</sup>, Anna Rohrbach<sup>2</sup>, and Marcus Rohrbach<sup>2</sup>

<sup>1</sup> TU Berlin, Germany

<sup>2</sup> TU Darmstadt & hessian.AI, Germany

<sup>3</sup> University of Edinburgh, UK

**Abstract.** Recent studies have shown promising results in utilizing multimodal large language models (MLLMs) for computer vision tasks such as object detection and semantic segmentation. However, many challenging video tasks remain under-explored. Video-language tasks necessitate spatial and temporal comprehension and require significant compute. Therefore, prior works have developed complex, highly specialized architectures or leveraged additional input signals such as video transcripts to best encode contextual and temporal information, which limits their generality and can be impractical. One particularly challenging task is video *moment retrieval*, which requires precise temporal and contextual grounding. This work demonstrates the surprising effectiveness of leveraging image-text pretrained MLLMs for moment retrieval. We introduce *Mr. BLIP* (Mr. as in Moment Retrieval), a multimodal, single-stage model that requires no expensive video-language pretraining, no additional input signal (e.g., no transcript or audio) and has a simpler and more versatile design than prior state-of-the-art methods. We achieve a new state-of-the-art in moment retrieval on the widely used benchmarks Charades-STA, QVHighlights, and ActivityNet Captions. Notably, we attain over 9% (absolute) higher Recall (at 0.5 and 0.7 IoU) on the challenging long-video multi-moment QVHighlights benchmark. Our code is publicly available <sup>1</sup>.

## 1 Introduction

The recent success of pretrained large language models (LLMs) [3, 14, 65] has inspired the development of generative image-text pretrained multimodal large language models (MLLMs) [1, 23, 36] that can comprehend vision and language modalities jointly. Furthermore, recent studies have demonstrated that large language models can be used as general-purpose interfaces [21] and can be adapted for image-based computer vision tasks such as object detection [9], image captioning [60], or visual grounding [47, 66]. However, due to higher computational and annotation costs, large-scale pretraining on video data is more challenging to scale. To circumvent the issue, recent studies leverage image-text pretrained models for image-to-video transfer learning [16, 25, 35, 42, 61, 62]. While such

---

<sup>1</sup> <https://github.com/sudo-Boris/mr-Blip>

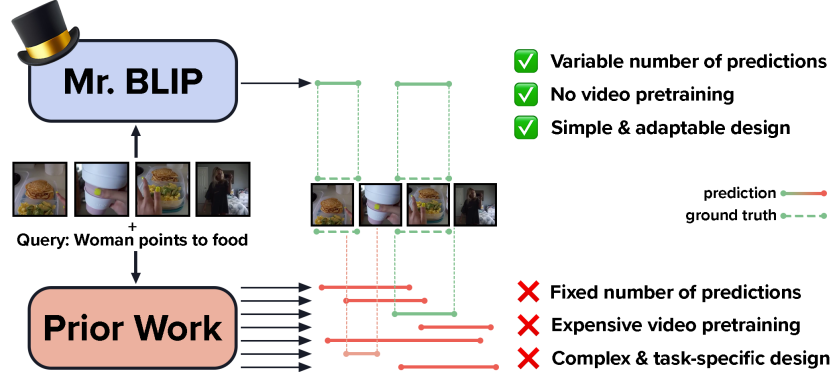


**Fig. 1: Advantages of *Mr. BLIP* over prior work.** In this work (top), we cast the task of predicting relevant windows based on a natural-language query as a sequence-to-sequence task. We utilize the frames directly and leverage an MLLM as a general-purpose interface [21] to predict a variable number of relevant moments that represent the query. In contrast, prior works (bottom) train static, task-specific multi-proposal prediction heads on top of a feature extractor to predict a fixed set of candidates and then sort the predicted moments based on a confidence score.

models offer promising results in the direction of video-text retrieval, video captioning, or multiple choice video question answering, generative MLLMs have not been extensively explored for video-based *moment retrieval*.

Video moment retrieval requires the precise temporal localization of all moments associated with an open-ended natural-language query in an untrimmed video. This task has multiple potential valuable applications, such as video search or indexing. More concretely, it requires understanding, discrimination, and temporal localization of multiple events in potentially minutes-long videos given an open-ended natural-language query. In the context of MLLMs, it is an open question of how to best model this task as a sequence-to-sequence prediction task, e.g., how to best represent timestamps so the model can reason about them and predict start and end timestamps correctly.

As illustrated in Fig. 1 (bottom), recent works generally approach the challenge of moment retrieval by leveraging an image-text aligned feature fusion module and train additional task-specific prediction heads that propose a fixed set of potentially relevant moment candidates. The final set of relevant moments is then selected from all candidates based on their confidence scores by picking the top- $k$  windows given  $k$  target windows in a benchmark. In practice, this approach is unsatisfactory, as selecting the right number of relevant windows given a fixed set of candidates is not trivial. Moreover, these methods often require expensive video pretraining to interpret the video modality.

In contrast, to the best of our knowledge, we are the first to cast the moment retrieval task as an open-ended sequence-to-sequence problem, leveraging a generative MLLM and demonstrating the surprising effectiveness of its context-

tual understanding abilities. This approach has two significant advantages. (1) We avoid the constraint of generating a fixed set of moment proposals (Fig. 1, bottom). Our model can predict a variable number of intervals that reflect the actual number of relevant moments, eliminating the ambiguity of selecting a subset of relevant moments given a fixed number of candidates (Fig. 1 top). (2) By leveraging an image-text pretrained MLLM we do not require expensive video pretraining and can quickly adapt to understanding the video modality.

In this work, we develop *Mr. BLIP* , an image-text pretrained, multimodal large language model based on BLIP-2 [36] and a novel multi-modal input sequence. The model design is capable of interpreting video data, and leverages interleaved temporal grounding of the input video signal (in the form of timestamps) to enhance its predictions. As illustrated in Fig. 1, we also start of with both visual frames and query. Prior work (bottom), often leverages video features [19] and CLIP [49] to then train a complex, task-specific feature fusion module that predicts a fixed set of candidates. In contrast, *Mr. BLIP* (top) leverages a sampled subset of the frames directly and utilizes the MLLM’s attention mechanism to learn the contextual and temporal relationship between visual frames, their interleaved temporal grounding, and the respective natural language query. Later in the paper, we discuss the relevance of deliberate design choices by conducting extensive ablation studies and demonstrate the surprising effectiveness of leveraging image-text pretrained MLLM for moment retrieval. Our approach achieves state-of-the-art results across the widely used benchmarks, Charades-STA [20], QVHighlights [33], and ActivityNet Captions [29].

In summary, our main contributions are the following: (i) We introduce *Mr. BLIP* for moment retrieval, leveraging image-text pretrained MLLMs by casting the moment retrieval task as an open-ended sequence-to-sequence problem. (ii) To enhance the temporal understanding of events in input videos, we design a novel multimodal input sequence. (iii) Our *Mr. BLIP* model improves the state-of-the-art across the most widely used moment retrieval benchmarks [20, 29, 33]. (iv) Finally, extensive experiments and ablations demonstrate the effectiveness of *Mr. BLIP* and its design choices. We find that representing time as absolute seconds and interleaving it with the respective frames yields the best performance.

## 2 Related Work

### 2.1 Moment Retrieval Models

Moment Retrieval analyzes an untrimmed video and aims to find the relevant clip for a given open-ended natural language query. Conventional approaches fall into either proposal-based or proposal-free methods. Proposal-based methods learn to identify moment candidates given predefined proposals, e.g., sliding windows [2, 20] and temporal anchors [8, 53], in a first stage. In a second stage, these candidates are further refined to better match the text query.

Proposal-free works include regression-based methods [33, 39, 46, 58, 63] that involve learning the interactions between both modalities to directly predict the

temporal boundaries of a relevant moment without the need for a first stage to generate initial proposals. Nevertheless, proposal-free methods still predict a fixed number of candidate windows alongside a confidence score.

The predicted windows are sorted based on the confidence score and are evaluated with proxy metrics based on different overlapping thresholds such as Recall@{0.5, 0.7}.

With the adoption of transformers and the success of the query-based design for object detection (DETR), recent works also employ this design for the moment retrieval task. Due to the slow and inefficient learning ability of moment queries, recent works have focused on initializing the queries with additional prior information [24] or developing complex attention modules [44, 45]. One of the state-of-the-art models, EaTR [24], utilizes pseudo event windows, obtained from the temporal self-similarity matrix (TSM) [26] and feeds them as positional queries. Conversely, our proposed design predicts moments without relying on any prior information. Furthermore, these models [44, 45] leverage 3D-temporal features such as Slow-Fast [19] or C3D [51] to predict a fixed set of moment candidates, as illustrated in Fig. 1 bottom. In contrast, we extract the individual frame features directly, omitting the reliance on expensive video-level features.

On the other hand, Yan *et al.* [58] leverage the large-scale image-text pre-trained CLIP [49] model for a unified video localization model. CLIP is used to encode video frames and text queries that are then concatenated and fed into a novel video-text fusion module based on the transformer [52] architecture with multiple prediction heads. This approach appears promising because it leverages language priors from the pretrained CLIP model early on in their model. Nevertheless, their approach requires expensive video pretraining on the Kinetics400 [27] and Kinetics700 [6] datasets. Finally, each prediction head is defined to solve a separate task: moment retrieval, action segmentation, and temporal action localization, respectively. In contrast, we leverage the strong contextual understanding ability of MLLMs by casting the moment retrieval task as an open-ended language modeling task and do not require any video pretraining. Similar to Yan *et al.* [58], our design also combines the language and vision context early on in the model so that the generation process is conditioned on both modalities from the beginning. Moreover, Luo *et al.* [41] also utilize image-text pretrained models but differ in methodology to *Mr. BLIP*. Their approach is metric learning based, focusing on moment retrieval by matching video and text, whereas ours is regression-based, directly predicting moment boundaries.

## 2.2 Computer Vision Tasks as Language Modeling

Recent works [9–13, 28, 37, 47, 55, 59, 60, 66] have demonstrated the possibility of casting various computer vision problems as language modeling tasks, addressing object detection [9, 48], semantic segmentation [30], or other vision-centric tasks [56]. In this work, we also cast temporal localization as a language modeling task. Unlike most previous work that focuses on image-level localization, similar to Yang *et al.* [59], we address the challenge of event localization in untrimmed

videos. However, we focus on moment retrieval, i.e., detecting moments in a video given a query, and not on dense event captioning.

Yu *et al.* [62] leverage BLIP-2 [36] for a naive approach to moment retrieval by iterating over the sampled subset of video frames and prompting the multi-modal large language model to classify each frame as relevant/irrelevant to the query of their downstream task. Yu *et al.* do not achieve state-of-the-art performance on the QVHighlights [33] but they hint at the possibility of leveraging MLLMs for moment retrieval tasks. Here, we explore this idea and extend it. We incorporate multiple frames and interleave their temporal grounding when constructing the input sequence to adapt BLIP-2 to understand their contextual and temporal relationship. We further fine-tune our model to output the retrieved moments in an open-ended sequence-to-sequence fashion and not only evaluate the probabilities of two tokens for binary classification (as in Yu *et al.*).

### 2.3 Image-to-Video Transfer Learning

The limited public availability of high-quality large-scale video-language datasets and immense compute requirements pose a significant challenge for large-scale video-language pretraining. The idea of leveraging image-language pretrained models for image-to-video transfer learning by utilizing a limited number of video frames to enhance learning efficiency has proven effective as evidenced by many recent publications [5, 16, 17, 25, 34, 35, 42, 43, 54, 57, 61, 62].

Yu *et al.* [61] leverage BLIP-2 [36] and the in-context learning abilities of MLLMs to fine-tune a model on egocentric videos using a fixed number of frames. An image-language pretrained MLLM allows them to train their model without requiring massive, naturalistic egocentric video datasets and transfer the image-language knowledge to the video-language modality.

Yu *et al.* [62] also make use of the contextual understanding of MLLMs to perform video question-answering tasks. The authors train a model to individually select 4 question-relevant frames and then prompt BLIP-2 using the separately obtained frame embeddings as context. The authors argue that performance decreases when providing more frames in the case of video question answering. We also leverage the pretrained BLIP-2 model and fine-tune it on a downstream video-language task, moment retrieval, but demonstrate strong performance improvements when providing significantly more frames as context.

## 3 *Mr. BLIP* for Moment Retrieval

The task of moment retrieval is to temporally localize all relevant moments in an untrimmed video given an open-ended natural language query. Therefore, a key challenge is to effectively model the contextual and temporal relationship between the different events in the video, for example, as illustrated in Fig. 2, a man is talking to the camera followed by him watching a show. Furthermore, due to the density of information in a video, it is computationally unfeasible to leverage all frames of a video as context in a single pass-through model.

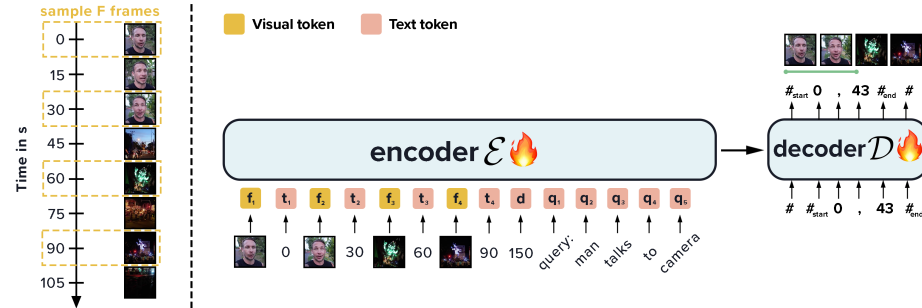


**Fig. 2: *Mr. BLIP* model overview.** We leverage a pretrained MLLM based on an encoder-decoder LLM such as BLIP-2 [36]. We sample  $F$  frames (left) and provide them separately as input to our LLM encoder  $\mathcal{E}$  (right). We construct the prompt for the LLM by concatenating the frame embeddings, the timestamps of each sampled frame, the video duration, the moment retrieval query, and a task prompt. (We do not visualize the task prompt for illustration purposes.) We finetune parts of the LLM leveraging parameter-efficient finetuning [22]. The LLM decoder  $\mathcal{D}$  outputs a sequence of potentially multiple retrieved moments by predicting the global BOS and EOS tokens, denoted by  $\#$ , the start of window and end of window tokens denoted as  $\#_{start}$  and  $\#_{end}$ , and the respective start and end times for each window.

To tackle these challenges, we cast moment retrieval as a language modeling task and leverage the contextual understanding ability of generative MLLMs to interpret and comprehend the semantic and temporal action development in frames that represent a video. We first design an MLLM-based multimodal model, *Mr. BLIP*, that can interpret video frames and their respective temporal grounding in the video and learn to associate a moment of the video to a natural language query (Section 3.1 and Fig. 2). Second, we develop a training strategy that effectively utilizes the limited amount of training data (Section 3.2).

### 3.1 Model

Our work explores the possibility of leveraging MLLMs capable of interpreting visual data for moment retrieval in videos given a natural language query. We design a model that can capture contextual and temporal relationships between the actions in an untrimmed video and the query. To do so, we cast the traditional moment retrieval task as an open-ended sequence-to-sequence problem, where we design a novel multimodal input sequence that contains (a) the visual semantic context given the sampled frames of the video, (b) the temporal context for each action given by the temporal grounding of each frame, and (c) the query in the form of a natural language description. The output of our model is a time interval sequence where each time interval represents a moment associated with the query and follows the formatting of a nested list containing potentially multiple moments with a start and end time.

As illustrated in Fig. 2, our architecture takes as visual input  $F$  sub-sampled video frames. There are multiple ways of modeling the temporal context for both input and output, which significantly affects the downstream performance. We find that modeling the timestamps as absolute seconds and, as visualized, interleaving them with the frames yields the best performance. With this representation, it is likely easier for the model to associate each frame  $f_i$  with its respective timestamp  $t_i$ .

**BLIP-2 Architecture.** We leverage the contextual understanding capabilities of MLLMs to interpret video data and detect relevant moments given an open-ended natural language query. To best leverage both the visual and the language signal, we adopt BLIP-2 [36] as the multimodal backbone for our model. BLIP-2 is a recent state-of-the-art MLLM pre-trained on a large image-text corpus. We leverage BLIP-2 to bootstrap the learning on video data, given its limited availability and expensive compute requirements for training. BLIP-2 comprises (1) a frozen image encoder [15, 18] combined with (2) a Q-Former, which is a trainable transformer [52] module that functions as a translation unit between the image encoder and the last component, and (3) a frozen LLM [14, 65].

**Multimodal sequence construction.** To model contextual and temporal relationships between the different actions in a video and a natural language query, we cast moment retrieval as a sequence-to-sequence task and develop a novel multimodal input sequence. It consists of frames  $f_n$ , timestamps  $t_n$  ( $n = 1, \dots, F$ ), video duration  $d$ , query  $q$  and task prompt  $p$  stating the task at hand as input. The task prompt we use is “*Given the video and the query, find the relevant windows. Relevant windows:*”. Finally, the model is tasked to predict the sequence of potentially multiple relevant windows  $m$ , which follows the formatting of a nested list of moments with a start and end time in seconds:  $y = [[t_{start}^1, t_{end}^1], [t_{start}^2, t_{end}^2], \dots]$ .

Notably, there are multiple ways of representing timestamps  $t_n$  and thus designing the multimodal sequence. Time can be represented in absolute or relative form, e.g., “79.9” seconds or “0.40” for a relative position; it could be a decimal number or be rounded to the nearest full integer value, e.g., “80” seconds or “40” for a relative position; the timestamps could be concatenated after the frames  $f_n$  or *interleaved* with them. As illustrated in Fig. 2, we find that representing time as simple text tokens of whole seconds (integer absolute form) and interleaving them with corresponding frames yields the best performance. We hypothesize this is the case because of how decimal numbers are tokenized. A decimal number, such as “79.9”, is tokenized into three tokens, whereas integers (up to “100”) are tokenized as a single token. One timestamp token corresponds to one frame. Additionally, placing each timestamp next to its associated frame aids the model to learn better which time token corresponds to which frame. In Sec. 4.2, we explore the different variations of representing time and concatenation of the different sequence elements of the input.

We find that representing timestamps as whole seconds (rounding decimal numbers to the nearest integer) and interleaving them with the frames yields the best performance. This finding leads to our final design for our multimodal input sequence  $x = [f_1, \text{round}(t_1), f_2, \text{round}(t_2), \dots, f_F, \text{round}(t_F), d, q, p]$ .

**Frame Encoder.** We denote BLIP-2’s frozen image encoder combined with Q-Former as our general-purpose frame encoder. The frame encoder is separately applied to each of the  $F$  sub-sampled frames, generating the frame embeddings and projecting them into the language space, yielding a shared embedding space. Prior works [59, 64] incorporate a further trainable transformer-based module to generate temporally and contextually correlated frame- or video-level embeddings. In contrast, we solely leverage the self- and cross-attention mechanisms of our LLM to learn the temporal and contextual relationships between frames.

**Text Decoder.** For the text decoder, we have chosen an encoder-decoder-based LLM. We leverage the instruction-trained Flan-T5 model [14] since the pretrained BLIP-2 frame encoder is aligned to it. The LLM encoder  $\mathcal{E}$  learns the correlation between the input sequence elements  $x = [f, t, d, q, p]$  due to its bi-directional attention mechanism and generates new multimodal contextualized output embeddings. The text decoder  $\mathcal{D}$  is based on a causal transformer decoder that cross-attends to the encoder outputs  $x$ . At each autoregressive step  $i$ , the decoder self-attends to the previously generated tokens  $\hat{m}_{<i}$  to output a conditioned probability distribution over the vocabulary of text:  $m_i = \mathcal{D}(\hat{m}_{<i}, \mathcal{E}(x)) \in \mathbb{R}^V$ , where  $V$  is the size of the vocabulary.

### 3.2 Training

In this section, we describe how we train our generative MLLM on the task of moment retrieval that has been cast from a traditional computer vision problem to an open-ended natural language sequence-to-sequence task.

**Parameter-Efficient Finetuning.** To train our model, we optimize for the standard maximum likelihood objective. Given the task input  $x$  and the decoder target text  $y$ , the objective is to minimize the following loss:

$$\mathcal{L}(x, y) = - \sum_{i=1}^{L-1} \log p_\theta(y_{i+1} | x, y_{1:i}), \quad (1)$$

where  $L$  is the length of the decoder target sequence and  $p_\theta$  denotes the output probability distribution over the vocabulary of text.

To further optimize training and best leverage the limited video data available, we implement parameter-efficient finetuning techniques, specifically LoRA [22], and randomly sample video frames. This allows us to only train roughly 20M parameters of the LLM, which is significantly less than in prior work [58, 59].

Additionally, by randomly sampling the frames, we optimize those weights by analyzing different frames and timestamps for the same videos each epoch. For further details on the random sampling, please refer to Appendix A.1.

### 3.3 Inference

At inference, we uniformly sample video frames to have the best temporal distribution. The text decoder then autoregressively generates the moment sequence by sampling from the model likelihood. In practice, we use beam search following prior work [59]. Finally, the natural language moment sequence is converted into a nested list of predicted moments interpreting the sequence as a common Python list, automatically fixing a few common formatting mistakes.

## 4 Experiments

This section describes the effectiveness of our design choices and compares our method to the state-of-the-art. In Section 4.1, we first elaborate on our experimental setup and implementation details. We then discuss our ablation studies in Section 4.2 and present our comparison to the state-of-the-art in Section 4.3. Finally, in Section 4.4, we show qualitative results from our approach.

### 4.1 Experimental Setup

**Benchmarks.** We validate *Mr. BLIP* on the three most widely used video moment retrieval (MR) datasets:

*Charades-STA* [20] includes 9,848 videos with an average duration of 30.6 seconds. The dataset contains 16,128 annotations with an average moment length of 8.1 seconds and an average query length of 7.22 words. The dataset is originally divided into two splits: training (12,408) and test (3,720). To avoid overfitting on the test set during training, we designate a part of the training set as a new validation set. The videos used in the validation set are not contained in the training set. Our new dataset split consists of a split for training, validation, and testing, with 11,166, 1,242, and 3,720 annotations, respectively. For a fair comparison, after completing our ablations, we train our final model on the original training set and report numbers on the test set.

*QVHighlights* [33] is one of the most recent benchmarks and contains 10,148 videos with a duration of 150 seconds. The videos were cropped out of YouTube videos, and each video is annotated with at least one query with an average length of 11.3 words describing the relevant moment. The target windows have an average length of 24.6 seconds. The dataset is split into training, validation, and test sets with 7,218, 1,150, and 1,542 queries, respectively. This benchmark is challenging because one query can be associated with multiple moments in a video. The test set targets are withheld and thus guarantee a fair benchmark.

The evaluation for the test split can only be measured through submitting the prediction to the evaluation server<sup>2</sup>.

*ActivityNet Captions* [29] contains 20,000 videos with an average duration of 2 minutes. The dataset contains 72,000 segments where each was human-annotated with a caption that contains on average 13.5 words. The dataset is divided into three splits, train (37,421), val\_1 (17,505), and val\_2 (17,031). Following [58], we use the train split for training, val\_1 for validation, and val\_2 for testing.

**Metrics.** The most commonly used metrics for MR are Recall@K and mean average precision (mAP) computed under different Intersection over Union (IoU) thresholds. The Recall@K metric is defined as the percentage of the top-K predicted segments having a larger temporal IoU than the threshold with a ground truth segment. Following the recent development [32, 33, 44, 45], we report the more challenging  $R1@0.5$  and  $R1@0.7$  scores, which correspond to the *Recall@1* scores at IoU thresholds of 0.5 and 0.7, respectively, and the mean IoU (mIoU) score. Following prior work, for MR on QVHighlights, we report the mAP score at IoU thresholds of 0.5 and 0.75, respectively.

**Implementation details.** Considering the relatively small scale of the datasets, we choose not to finetune the entire 3 billion parameter-LLM backbone of our model but rather leverage parameter-efficient finetuning [22] to train only 19 million parameters, as described in Section 3.2.

Since our objective is a generative language modeling task, our model can output minor formatting inconsistencies that would invalidate the prediction if not treated otherwise. Similar to [59], we post-process the model’s outputs by applying heuristics to clean up minor flaws in the prediction.

For Charades-STA, we extract 20 video frames for each video, which is significantly less than prior work which requires 128 frames [58]. We train for up to 50 epochs with a batch size of 32 samples split across 4 A100-80GB GPUs for about 55 GPU hours. For QVHighlights and ActivityNet Captions, we extract 60 video frames for each video, which is less than required by prior work. We train for up to 50 epochs with an effective batch size of 32 samples by splitting them across 8 A100-80-GB GPUs and leveraging accumulated gradients set to 4 (i.e., we have one sample per GPU), and train for about 170 GPU hours.

We start with a learning rate (lr) of 1e-8, perform linear lr warmup to 3e-4 for 10% of the total number of iterations and then apply a cosine lr decay. We utilize the AdamW [40] optimizer and sample the frames randomly during training.

## 4.2 Ablation Studies

By default, our *Mr. BLIP* models for Charades-STA (QVHighlights/ ANet Captions) leverage 20 (60) visual frames, their associated timestamps, video duration, a query, and a task prompt. If not stated otherwise, we represent time as

---

<sup>2</sup> Evaluation server, QVHighlights: <https://codalab.lisn.upsaclay.fr/competitions/6937>

**Table 1: Ablation on design of prompt.** Evaluation on Charades-STA.

Input components	R1@0.5	R1@0.7	mIoU
Frames only	43.89	23.47	41.25
+ Duration	58.28	34.00	51.01
+ Frame timestamps	67.28	45.26	57.24
+ Task description	<b>67.28</b>	<b>46.7</b>	<b>57.46</b>

**Table 2: Design of timestamps.** We demonstrate the importance of how we represent time: (A) Representing time as decimal numbers has the lowest performance while providing absolute timestamps improves the performance over relative temporal positions. (B) Interleaving frames with their associated timestamps yields further significant improvement. The ablation was done on the Charades-STA validation set.

#	Representation	Precision	Interleaved	R1@0.5	R1@0.7	mIoU
(1)	Relative	decimal	<b>✗</b>	62.30	37.22	54.03
(2)	Absolute	decimal	<b>✗</b>	62.38	36.33	53.59
(3)	Relative	integer	<b>✗</b>	63.10	36.01	53.86
(4)	Absolute	integer	<b>✗</b>	64.39	41.80	56.00
(5)	Relative	integer	<b>✓</b>	65.19	44.94	56.99
(6)	Absolute	integer	<b>✓</b>	<b>67.28</b>	<b>46.70</b>	<b>57.46</b>

simple text tokens of whole seconds and interleave these with frame tokens. In the following, we ablate the impact of these design choices on the downstream moment retrieval performance by reporting results on our Charades-STA validation set.

**Design of sequence.** In Table 1, we analyze the effectiveness of each part of the multimodal input sequence of our MLLM, by cumulatively adding each component starting with only providing the frames. The query is always part of the sequence. Adding the video duration, in addition to the visual inputs, improves the downstream performance significantly (row 2 vs. row 1). This shows the importance of providing the model a point of reference to infer the temporal location of each frame and demonstrates the ability of the MLLM to learn this association. Furthermore, additionally providing the specific timestamps at which each frame was sampled improves the model performance even further by a significant margin (row 3 vs. row 2). This demonstrates the relevance of designing the input context to provide as much relevant information as possible, while still not relying on additional computation such as generating and leveraging transcripts. Finally, we surprisingly find that adding a task prompt describing what we expect the model to do ("*Given the video and the query, find the relevant windows. Relevant windows:* ") improves model performance as well (row 4 vs. row 3) and might be worth exploring in future work. We hypothesize this is due to the instruction tuning in our leveraged Flan-T5 [14] model.

**Table 3: Ablation on the number of input frames.** Evaluation on Charades-STA eval.

#Frames	R1@0.5	R1@0.7	mIoU
5	54.50	32.72	48.26
10	64.63	41.80	55.81
15	67.79	44.07	57.71
20	67.28	<b>46.70</b>	57.46
25	<b>67.95</b>	43.35	<b>57.91</b>
30	64.58	41.51	55.79

**Design of timestamps.** A central question for this work is how MLLMs can best represent and reason about timestamps, as they have to be interpreted in the input and predicted in the output. We compare different options for representing the timestamps and their impact on the final downstream model performance. We explore using relative positions w.r.t the video duration vs. representing each timestamp as absolute time. In both cases, we explore representing the numbers as decimal numbers, e.g., “79.9” seconds or “0.40” for a relative position, and whole integers, e.g., “80” seconds or “40” for a relative position. In these experiments, the format of the timestamps in model input and output is always consistent. In the case of relative positions, we post-process the output to yield an absolute value to compare to the ground truth for the final evaluation.

In Table 2 we observe, that that representing the timestamps in decimal form results in lower performance for both absolute and relative form, see rows (1,2) vs. rows (3, 4). We hypothesize this is the case because of how decimal numbers are tokenized. A decimal number, such as “79.9”, is tokenized into three tokens, whereas integers (up to “100”) are all tokenized as one token. This shows the importance of designing the input and outputs with the representation of the MLLM in mind. Further, we observe that absolute position in seconds yields better performance than the relative representation when using integer precision.

Finally, we explore the design choice of ordering frame and time tokens. In rows (1) through (4), we concatenate all frames together, followed by a concatenation of the timestamps, which are each separated by a separator token (“>”). In rows (5) and (6), we demonstrate the benefit of *interleaving* frame tokens with time tokens so that each frame is followed by its respective timestamp representation (as illustrated in Fig. 2). This again shows the importance of a careful prompt design. We hypothesize that the attention mechanism can more easily learn the correlation between a frame and its associated timestamp.

**Number of input frames.** In Table 3, we show the impact of the number of input frames and demonstrate the ability of our image-text pretrained MLLM to adapt to the video modality.

For Charades-STA with an average video duration of 30 seconds, using 20 frames achieves the highest performance on R1@0.7, improving over 15 frames

**Table 4: Comparison with state-of-the-art.** Charades-STA [20], QVHighlights [33], and ActivityNet Captions [29]. **CLIP\***: UnLoc [58] pretrains the backbone with action classification datasets Kinetics 400/700. **SF**: Slow-Fast backbone. Discussion in the main text.

Method	Backbone	mIoU	R1@.5	R1@.7	mAP@.5	mAP@.75
<b>QVHighlights [33]</b> Validation set						
EaTR [24]	I3D	–	61.36	45.79	61.86	41.91
UnLoc-L [58]	CLIP*	–	66.10	46.70	–	–
<i>Mr. BLIP</i> 	BLIP-2	–	<b>76.13</b>	<b>63.35</b>	<b>69.39</b>	<b>55.78</b>
<b>QVHighlights [33]</b> Test set						
SeViLa [62]	BLIP-2	–	54.50	36.50	–	–
UniVTG [38]	SF+CLIP	–	58.86	40.86	57.60	35.59
QD-DETR [45]	SF+CLIP	–	62.40	44.98	62.52	39.88
CG-DETR [44]	SF+CLIP	–	65.43	48.38	64.51	42.77
<i>Mr. BLIP</i> 	BLIP-2	–	<b>74.77</b>	<b>60.51</b>	<b>68.12</b>	<b>53.38</b>
<b>Charades-STA [20]</b> Test set						
UniVTG [38]	SF+CLIP	50.10	58.01	35.65	–	–
QD-DETR [45]	SF+CLIP	–	57.31	32.55	–	–
CG-DETR [44]	SF+CLIP	50.13	58.44	36.34	–	–
UnLoc-L [58]	CLIP*	–	60.80	38.40	–	–
EaTR [24]	I3D	–	68.47	44.92	–	–
<i>Mr. BLIP</i> 	BLIP-2	<b>58.63</b>	<b>69.31</b>	<b>49.29</b>	–	–
<b>ActivityNet Captions [29]</b> Single sentence MR. Test set						
VLG [50]	GCNeXt	–	46.30	29.80	–	–
UnLoc-L [58]	CLIP*	–	48.30	30.20	–	–
<i>Mr. BLIP</i> 	BLIP-2	–	<b>53.92</b>	<b>35.55</b>	–	–

by 2.63% and over 25 frames by 2.25%, respectively. We observe, that inputting 25 frames does improve the R1@.5 and mIoU scores compared to leveraging 20 frames, but only by 0.67% and 0.45%, respectively while increasing compute requirements. Leveraging 30 frames reduces the performance, albeit theoretically adding more information.

The number of input frames is a hyperparameter that we explore for each dataset on the validation set. For QVHighlights, which consists of 150-second long videos, and for ActivityNet, which on average has 120-second long videos, we have found 60 frames to perform the best, showing the ability of *Mr. BLIP* to comprehend a relatively long sequence of interleaved visual and textual tokens.

### 4.3 Comparison to the State-of-the-Art

Next, we compare *Mr. BLIP* to the state-of-the-art (SoTA) approaches for MR following the best design choices derived from our ablations in Section 4.2.

**Moment Retrieval** As outlined in Table 4, for QVHighlights, *Mr. BLIP* significantly outperforms the previous SoTA [44] on all metrics. Our model improves the performance by 9.21%, 11.41%, 3.9%, and 10.18% for R1@0.5, R1@0.7, mAP@0.5, and mAP@0.75, respectively. Interestingly, we find that the improvement on the more difficult metrics (with a higher IoU threshold) is higher than on the easier metrics (with a lower IoU threshold). This implies that our model may not only predict significantly more acceptable windows, i.e., windows with an IoU>0.5, but a larger subset of those have a higher precision, indicated by the even larger improvements for IoU>0.7 and IoU>0.75, respectively.

Notably, we also outperform the best reported approach on QVHighlights validation set, UnLoc-L [58], with far fewer input frames, 128 vs. 20, and without expensive video pretraining of the backbone.

As shown in Table 4, on Charades-STA, our *Mr. BLIP* model achieves a new state-of-the-art improving over the previous SoTA model [24]. While [24] performs well on Charades-STA, it underperforms significantly on QVHighlights (e.g., about 17% drop on R1@0.7 compared to *Mr. BLIP*), highlighting the generality of our approach.

Furthermore, as shown in Table 4, *Mr. BLIP* outperforms the previous SoTA [58] in moment retrieval on ActivityNet Captions by 5.62% and 5.35% on R1@0.5 and R1@0.7, respectively.

Most previous works build upon features that were pre-extracted by convolutional neural networks [31], such as I3D [7] or Slow-Fast [19], often in combination with CLIP [49], with one recent state-of-the-art model, UnLoc [58], being the first to build solely on the image-text pretrained CLIP. Our work is most comparable to SeViLa [62], which leverages the same image-text pretrained MLLM, namely BLIP-2 [36], as its backbone. Our *Mr. BLIP* model achieves performance that is 20.14% and 23.29% higher than SeViLa on QVHighlights in Recall@1 at thresholds of IoU=0.5 and IoU=0.7. This demonstrates the effectiveness of our novel multimodal sequence design. We provide contextual and temporal information to our model and have it predict the relevant moments in a single, autoregressive pass-through. In contrast, SeViLa classifies each frame as relevant to the query or not, without any contextual and temporal information about the video.

To the best of our knowledge, ours is the first work casting the task of moment retrieval as an open-ended sequence-to-sequence problem and leveraging a generative MLLM that achieves the new state-of-the-art results on moment retrieval, which has been largely dominated by complex task-specific architectures.

#### 4.4 Qualitative Results

In this section, we analyze qualitative results illustrated in Fig. 3.

In examples 1, 2, and 3, we observe the ability of *Mr. BLIP* to successfully localize one or multiple moments given a natural language query. Example 4 represents a case where our model predicts two correct moments alongside one that is false. Example 5 shows a failure case, in which our model predicts a moment where the woman is clearly visible in a shop but not trying on a hat.

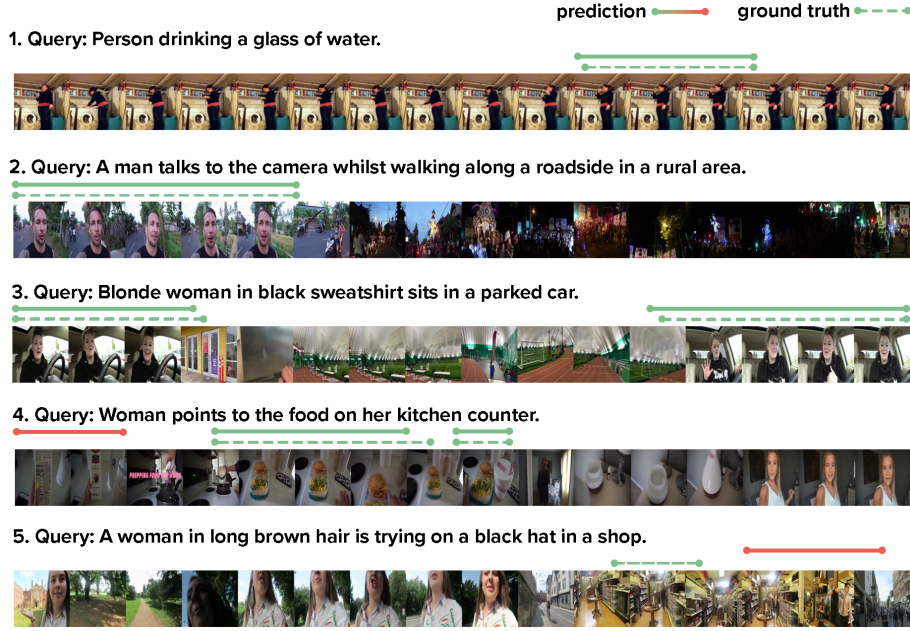


**Fig. 3: Qualitative results.** We showcase several example predictions from our *Mr. BLIP* model, including success and failure cases. Example 1 is from Charades-STA and examples 2-5 are from QVHighlights. Discussion in the main text.

In the ground truth segment, the woman is trying on a hat but is not clearly visible since she is far away.

## 5 Conclusion

We introduce *Mr. BLIP*, a multimodal large language model that performs moment retrieval by generating a variable number of relevant windows as a single sequence of text tokens given multimodal inputs. We show that *Mr. BLIP* does not require expensive video pretraining and greatly benefits from an input design that incorporates visual and temporal information as a simple interleaved token sequence of visual and text tokens. *Mr. BLIP* achieves state-of-the-art results on the most common moment retrieval benchmarks while leveraging a highly versatile design that allows for simple extension to further tasks. We hope this versatile sequence-to-sequence design of *Mr. BLIP* sparks further research in leveraging large-scale image-text pretrained MLLMs for computer-vision-based video understanding tasks.

A potentially interesting area to analyze is the impact and utility of the task prompt. It might be worth exploring training our model to handle multi-task problems and defining the output of *Mr. BLIP* via the task prompt.

**Limitations and Impact.** Since we leverage a large-scale pretrained MLLM, BLIP-2 [36], we can not rule out the presence of any biases or harmful stereotypes (e.g., gender or racial biases) that BLIP-2 has learned. It is conceivable that our model will detect moments that fall into the category of harmful stereotypes. We recommend applying our model with caution when adopting it in practice. Moreover, our model could be subject to misuse w.r.t some forms of surveillance.

**Acknowledgements.** As part of their affiliation with TU Darmstadt, the research of BM and MR was funded, in part, by a LOEWE-Spitzen-Professur (LOEWE/4a//519/ 05.00.002-(0010)/93) and an Alexander von Humboldt Professorship in Multimodal Reliable AI sponsored by Germany’s Federal Ministry for Education and Research.

## References

1. Alayrac, J.B., Donahue, J., Luc, P., Miech, A., Barr, I., Hasson, Y., Lenc, K., Mensch, A., Millican, K., Reynolds, M., et al.: Flamingo: a visual language model for few-shot learning. In: Advances in Neural Information Processing Systems. vol. 35, pp. 23716–23736 (2022) 1
2. Anne Hendricks, L., Wang, O., Shechtman, E., Sivic, J., Darrell, T., Russell, B.: Localizing moments in video with natural language. In: Proceedings of the IEEE international conference on computer vision. pp. 5803–5812 (2017) 3
3. Brown, T., Mann, B., Ryder, N., Subbiah, M., Kaplan, J.D., Dhariwal, P., Neelakantan, A., Shyam, P., Sastry, G., Askell, A., et al.: Language models are few-shot learners. In: Advances in neural information processing systems. vol. 33, pp. 1877–1901 (2020) 1
4. Caba Heilbron, F., Escorcia, V., Ghanem, B., Carlos Niebles, J.: Activitynet: A large-scale video benchmark for human activity understanding. In: Proceedings of the IEEE Conference on Computer Vision and Pattern Recognition (CVPR) (June 2015) 21
5. Cao, M., Yang, T., Weng, J., Zhang, C., Wang, J., Zou, Y.: Locvtp: Video-text pre-training for temporal localization. In: European Conference on Computer Vision. pp. 38–56. Springer (2022) 5
6. Carreira, J., Noland, E., Hillier, C., Zisserman, A.: A short note on the kinetics-700 human action dataset. arXiv preprint arXiv:1907.06987 (2019) 4
7. Carreira, J., Zisserman, A.: Quo vadis, action recognition? a new model and the kinetics dataset. In: proceedings of the IEEE Conference on Computer Vision and Pattern Recognition. pp. 6299–6308 (2017) 14
8. Chen, J., Chen, X., Ma, L., Jie, Z., Chua, T.S.: Temporally grounding natural sentence in video. In: Proceedings of the 2018 conference on empirical methods in natural language processing. pp. 162–171 (2018) 3
9. Chen, T., Saxena, S., Li, L., Fleet, D.J., Hinton, G.: Pix2seq: A language modeling framework for object detection. In: International Conference on Learning Representations (2022) 1, 4
10. Chen, T., Saxena, S., Li, L., Lin, T.Y., Fleet, D.J., Hinton, G.E.: A unified sequence interface for vision tasks. In: Advances in Neural Information Processing Systems. vol. 35, pp. 31333–31346 (2022) 4

11. Chen, X., Wang, X., Changpinyo, S., Piergiovanni, A., Padlewski, P., Salz, D., Goodman, S., Grycner, A., Mustafa, B., Beyer, L., et al.: Pali: A jointly-scaled multilingual language-image model. In: International Conference on Learning Representations (2023) [4](#)
12. Chen, Z., Zhu, Y., Li, Z., Yang, F., Li, W., Wang, H., Zhao, C., Wu, L., Zhao, R., Wang, J., et al.: Obj2seq: Formatting objects as sequences with class prompt for visual tasks. In: Advances in Neural Information Processing Systems. vol. 35, pp. 2494–2506 (2022) [4](#)
13. Cho, J., Lei, J., Tan, H., Bansal, M.: Unifying vision-and-language tasks via text generation. In: International Conference on Machine Learning. pp. 1931–1942. PMLR (2021) [4](#)
14. Chung, H.W., Hou, L., Longpre, S., Zoph, B., Tay, Y., Fedus, W., Li, Y., Wang, X., Dehghani, M., Brahma, S., et al.: Scaling instruction-finetuned language models. arXiv preprint arXiv:2210.11416 (2022) [1](#), [7](#), [8](#), [11](#)
15. Dosovitskiy, A., Beyer, L., Kolesnikov, A., Weissenborn, D., Zhai, X., Unterthiner, T., Dehghani, M., Minderer, M., Heigold, G., Gelly, S., et al.: An image is worth 16x16 words: Transformers for image recognition at scale. In: International Conference on Learning Representations (2021) [7](#)
16. Fang, H., Xiong, P., Xu, L., Chen, Y.: Clip2video: Mastering video-text retrieval via image clip. arXiv preprint arXiv:2106.11097 (2021) [1](#), [5](#)
17. Fang, H., Xiong, P., Xu, L., Luo, W.: Transferring image-clip to video-text retrieval via temporal relations. IEEE Transactions on Multimedia (2022) [5](#)
18. Fang, Y., Wang, W., Xie, B., Sun, Q., Wu, L., Wang, X., Huang, T., Wang, X., Cao, Y.: Eva: Exploring the limits of masked visual representation learning at scale. In: Proceedings of the IEEE/CVF Conference on Computer Vision and Pattern Recognition. pp. 19358–19369 (2023) [7](#)
19. Feichtenhofer, C., Fan, H., Malik, J., He, K.: Slowfast networks for video recognition. In: Proceedings of the IEEE/CVF international conference on computer vision. pp. 6202–6211 (2019) [3](#), [4](#), [14](#)
20. Gao, J., Sun, C., Yang, Z., Nevatia, R.: Tall: Temporal activity localization via language query. In: Proceedings of the IEEE international conference on computer vision. pp. 5267–5275 (2017) [3](#), [9](#), [13](#), [21](#), [22](#)
21. Hao, Y., Song, H., Dong, L., Huang, S., Chi, Z., Wang, W., Ma, S., Wei, F.: Language models are general-purpose interfaces. arXiv preprint arXiv:2206.06336 (2022) [1](#), [2](#)
22. Hu, E.J., Shen, Y., Wallis, P., Allen-Zhu, Z., Li, Y., Wang, S., Wang, L., Chen, W.: Lora: Low-rank adaptation of large language models. In: International Conference on Learning Representations (2022) [6](#), [8](#), [10](#), [22](#)
23. Huang, S., Dong, L., Wang, W., Hao, Y., Singhal, S., Ma, S., Lv, T., Cui, L., Mohammed, O.K., Patra, B., et al.: Language is not all you need: Aligning perception with language models. In: Advances in Neural Information Processing Systems. vol. 36 (2024) [1](#)
24. Jang, J., Park, J., Kim, J., Kwon, H., Sohn, K.: Knowing where to focus: Event-aware transformer for video grounding. In: Proceedings of the IEEE/CVF International Conference on Computer Vision. pp. 13846–13856 (2023) [4](#), [13](#), [14](#)
25. Ju, C., Han, T., Zheng, K., Zhang, Y., Xie, W.: Prompting visual-language models for efficient video understanding. In: European Conference on Computer Vision. pp. 105–124. Springer (2022) [1](#), [5](#)
26. Kang, H., Kim, J., Kim, T., Kim, S.J.: Uboco: Unsupervised boundary contrastive learning for generic event boundary detection. In: Proceedings of the IEEE/CVF

Conference on Computer Vision and Pattern Recognition. pp. 20073–20082 (2022) [4](#)

27. Kay, W., Carreira, J., Simonyan, K., Zhang, B., Hillier, C., Vijayanarasimhan, S., Viola, F., Green, T., Back, T., Natsev, P., et al.: The kinetics human action video dataset. arXiv preprint arXiv:1705.06950 (2017) [4](#)

28. Kolesnikov, A., Susano Pinto, A., Beyer, L., Zhai, X., Harmsen, J., Houlsby, N.: Uvim: A unified modeling approach for vision with learned guiding codes. In: Advances in Neural Information Processing Systems. vol. 35, pp. 26295–26308 (2022) [4](#)

29. Krishna, R., Hata, K., Ren, F., Fei-Fei, L., Carlos Niebles, J.: Dense-captioning events in videos. In: Proceedings of the IEEE international conference on computer vision. pp. 706–715 (2017) [3, 10, 13, 21](#)

30. Lai, X., Tian, Z., Chen, Y., Li, Y., Yuan, Y., Liu, S., Jia, J.: Lisa: Reasoning segmentation via large language model. In: Proceedings of the IEEE/CVF Conference on Computer Vision and Pattern Recognition. pp. 9579–9589 (2024) [4](#)

31. LeCun, Y., Boser, B., Denker, J., Henderson, D., Howard, R., Hubbard, W., Jackel, L.: Handwritten digit recognition with a back-propagation network. In: Touretzky, D. (ed.) Advances in Neural Information Processing Systems. vol. 2. Morgan-Kaufmann (1989) [14](#)

32. Lee, P., Byun, H.: Bam-detr: Boundary-aligned moment detection transformer for temporal sentence grounding in videos. arXiv preprint arXiv:2312.00083 (2023) [10](#)

33. Lei, J., Berg, T.L., Bansal, M.: Detecting moments and highlights in videos via natural language queries. In: Advances in Neural Information Processing Systems. vol. 34, pp. 11846–11858 (2021) [3, 5, 9, 10, 13, 21, 22](#)

34. Lei, J., Berg, T.L., Bansal, M.: Revealing single frame bias for video-and-language learning. In: Annual Meeting of the Association for Computational Linguistics (2022) [5](#)

35. Lei, J., Li, L., Zhou, L., Gan, Z., Berg, T.L., Bansal, M., Liu, J.: Less is more: Clipbert for video-and-language learning via sparse sampling. In: Proceedings of the IEEE/CVF conference on computer vision and pattern recognition. pp. 7331–7341 (2021) [1, 5](#)

36. Li, J., Li, D., Savarese, S., Hoi, S.: Blip-2: bootstrapping language-image pre-training with frozen image encoders and large language models. In: Proceedings of the 40th International Conference on Machine Learning. ICML'23, JMLR.org (2023) [1, 3, 5, 6, 7, 14, 16](#)

37. Li, W., Cao, Z., Feng, J., Zhou, J., Lu, J.: Label2label: A language modeling framework for multi-attribute learning. In: European Conference on Computer Vision. pp. 562–579. Springer (2022) [4](#)

38. Lin, K.Q., Zhang, P., Chen, J., Pramanick, S., Gao, D., Wang, A.J., Yan, R., Shou, M.Z.: Univtg: Towards unified video-language temporal grounding. In: Proceedings of the IEEE/CVF International Conference on Computer Vision. pp. 2794–2804 (2023) [13](#)

39. Liu, Y., Li, S., Wu, Y., Chen, C.W., Shan, Y., Qie, X.: Umt: Unified multi-modal transformers for joint video moment retrieval and highlight detection. In: Proceedings of the IEEE/CVF Conference on Computer Vision and Pattern Recognition. pp. 3042–3051 (2022) [3](#)

40. Loshchilov, I., Hutter, F.: Decoupled weight decay regularization. arXiv preprint arXiv:1711.05101 (2017) [10](#)

41. Luo, D., Huang, J., Gong, S., Jin, H., Liu, Y.: Towards generalisable video moment retrieval: Visual-dynamic injection to image-text pre-training. In: Proceedings of

the IEEE/CVF Conference on Computer Vision and Pattern Recognition (CVPR). pp. 23045–23055 (June 2023) 4

42. Luo, H., Ji, L., Zhong, M., Chen, Y., Lei, W., Duan, N., Li, T.: Clip4clip: An empirical study of clip for end to end video clip retrieval and captioning. *Neurocomputing* **508**, 293–304 (2022) 1, 5
43. Ma, Y., Xu, G., Sun, X., Yan, M., Zhang, J., Ji, R.: X-clip: End-to-end multi-grained contrastive learning for video-text retrieval. In: Proceedings of the 30th ACM International Conference on Multimedia. pp. 638–647 (2022) 5
44. Moon, W., Hyun, S., Lee, S., Heo, J.P.: Correlation-guided query-dependency calibration in video representation learning for temporal grounding. arXiv preprint arXiv:2311.08835 (2023) 4, 10, 13, 14
45. Moon, W., Hyun, S., Park, S., Park, D., Heo, J.P.: Query-dependent video representation for moment retrieval and highlight detection. In: Proceedings of the IEEE/CVF Conference on Computer Vision and Pattern Recognition. pp. 23023–23033 (2023) 4, 10, 13
46. Mun, J., Cho, M., Han, B.: Local-global video-text interactions for temporal grounding. In: Proceedings of the IEEE/CVF Conference on Computer Vision and Pattern Recognition. pp. 10810–10819 (2020) 3
47. Peng, Z., Wang, W., Dong, L., Hao, Y., Huang, S., Ma, S., Wei, F.: Grounding multimodal large language models to the world. In: International Conference on Learning Representations (2024) 1, 4
48. Pi, R., Gao, J., Diao, S., Pan, R., Dong, H., Zhang, J., Yao, L., Han, J., Xu, H., Kong, L., et al.: Detgpt: Detect what you need via reasoning. arXiv preprint arXiv:2305.14167 (2023) 4
49. Radford, A., Kim, J.W., Hallacy, C., Ramesh, A., Goh, G., Agarwal, S., Sastry, G., Askell, A., Mishkin, P., Clark, J., et al.: Learning transferable visual models from natural language supervision. In: International conference on machine learning. pp. 8748–8763. PMLR (2021) 3, 4, 14
50. Soldan, M., Xu, M., Qu, S., Tegner, J., Ghanem, B.: Vlg-net: Video-language graph matching network for video grounding. In: Proceedings of the IEEE/CVF International Conference on Computer Vision. pp. 3224–3234 (2021) 13
51. Tran, D., Bourdev, L., Fergus, R., Torresani, L., Paluri, M.: Learning spatiotemporal features with 3d convolutional networks. In: Proceedings of the IEEE international conference on computer vision. pp. 4489–4497 (2015) 4
52. Vaswani, A., Shazeer, N., Parmar, N., Uszkoreit, J., Jones, L., Gomez, A.N., Kaiser, Ł., Polosukhin, I.: Attention is all you need. In: Advances in neural information processing systems. vol. 30 (2017) 4, 7
53. Wang, J., Ma, L., Jiang, W.: Temporally grounding language queries in videos by contextual boundary-aware prediction. In: Proceedings of the AAAI Conference on Artificial Intelligence. vol. 34, pp. 12168–12175 (2020) 3
54. Wang, J., Ge, Y., Cai, G., Yan, R., Lin, X., Shan, Y., Qie, X., Shou, M.Z.: Object-aware video-language pre-training for retrieval. In: Proceedings of the IEEE/CVF conference on computer vision and pattern recognition. pp. 3313–3322 (2022) 5
55. Wang, P., Yang, A., Men, R., Lin, J., Bai, S., Li, Z., Ma, J., Zhou, C., Zhou, J., Yang, H.: Ofa: Unifying architectures, tasks, and modalities through a simple sequence-to-sequence learning framework. In: International Conference on Machine Learning. pp. 23318–23340. PMLR (2022) 4
56. Wang, W., Chen, Z., Chen, X., Wu, J., Zhu, X., Zeng, G., Luo, P., Lu, T., Zhou, J., Qiao, Y., et al.: Visionllm: Large language model is also an open-ended decoder for vision-centric tasks. Advances in Neural Information Processing Systems **36** (2024) 4

57. Xue, H., Sun, Y., Liu, B., Fu, J., Song, R., Li, H., Luo, J.: Clip-vip: Adapting pre-trained image-text model to video-language representation alignment. In: International Conference on Learning Representations (2023) [5](#)
58. Yan, S., Xiong, X., Nagrani, A., Arnab, A., Wang, Z., Ge, W., Ross, D., Schmid, C.: Unloc: A unified framework for video localization tasks. In: Proceedings of the IEEE/CVF International Conference on Computer Vision. pp. 13623–13633 (2023) [3](#), [4](#), [8](#), [10](#), [13](#), [14](#)
59. Yang, A., Nagrani, A., Seo, P.H., Miech, A., Pont-Tuset, J., Laptev, I., Sivic, J., Schmid, C.: Vid2seq: Large-scale pretraining of a visual language model for dense video captioning. In: Proceedings of the IEEE/CVF Conference on Computer Vision and Pattern Recognition. pp. 10714–10726 (2023) [4](#), [8](#), [9](#), [10](#)
60. Yang, Z., Gan, Z., Wang, J., Hu, X., Ahmed, F., Liu, Z., Lu, Y., Wang, L.: Unitab: Unifying text and box outputs for grounded vision-language modeling. In: European Conference on Computer Vision. pp. 521–539. Springer (2022) [1](#), [4](#)
61. Yu, K.P., Zhang, Z., Hu, F., Chai, J.: Efficient in-context learning in vision-language models for egocentric videos. arXiv preprint arXiv:2311.17041 (2023) [1](#), [5](#)
62. Yu, S., Cho, J., Yadav, P., Bansal, M.: Self-chained image-language model for video localization and question answering. In: Advances in Neural Information Processing Systems. vol. 36 (2024) [1](#), [5](#), [13](#), [14](#)
63. Zeng, R., Xu, H., Huang, W., Chen, P., Tan, M., Gan, C.: Dense regression network for video grounding. In: Proceedings of the IEEE/CVF Conference on Computer Vision and Pattern Recognition. pp. 10287–10296 (2020) [3](#)
64. Zhang, H., Li, X., Bing, L.: Video-LLaMA: An instruction-tuned audio-visual language model for video understanding. In: Feng, Y., Lefever, E. (eds.) Proceedings of the 2023 Conference on Empirical Methods in Natural Language Processing: System Demonstrations. pp. 543–553. Association for Computational Linguistics, Singapore (Dec 2023) [8](#)
65. Zhang, S., Roller, S., Goyal, N., Artetxe, M., Chen, M., Chen, S., Dewan, C., Diab, M., Li, X., Lin, X.V., et al.: Opt: Open pre-trained transformer language models. arXiv preprint arXiv:2205.01068 (2022) [1](#), [7](#)
66. Zhu, C., Zhou, Y., Shen, Y., Luo, G., Pan, X., Lin, M., Chen, C., Cao, L., Sun, X., Ji, R.: Seqtr: A simple yet universal network for visual grounding. In: European Conference on Computer Vision. pp. 598–615. Springer (2022) [1](#), [4](#)

**Table 5:** Hyperparameters for our base models for Charades-STA [20], QVHighlights (QVH) [33], and ActivityNet (ANet) [4, 29].

Hyperparameter	Charades-STA	QVH/ ANet
Batch size	32	32
Epochs	50	50
Learning rate	3e-4	3e-4
Learning rate warmup	Linear	Linear
Learning rate warmup steps	10%	10%
Learning rate decay	Cosine	Cosine
Optimizer	AdamW	AdamW
Weight decay	0.05	0.05
# input frames	20	60
# beams	5	5

## A Implementation Details

### A.1 Video processing

We build on top of the Salesforce [lavis](#) repository and leverage their implementation of randomly and uniformly extracting frames from a video. During training, we randomly sample frames as a means of data augmentation to alter the frames seen by the model in each batch. At inference, we sample uniformly to provide an equal coverage of the entire video. For random sampling, we start by uniformly extracting  $n+1$  timestamps, where the first and last timestamps are at  $t = 0$  and  $t = \text{video\_length}$ , respectively. Afterward, we randomly sample one frame between each pair of adjacent timestamps, yielding the final  $n$  randomly sampled frames. This process of random sampling can be considered adding noise to a uniform sampling process.

During training, we randomly crop and resize each frame to 224x224 pixels. We then normalize each frame by subtracting by a fixed mean and dividing by a specified standard deviation. At inference, we don't apply random cropping and resizing. We only apply the normalization.

### A.2 Hyperparameters

Table 5 shows a detailed list of hyperparameters. To ensure a fair comparison for all our models and ablations, we stick to hyperparameters presented in the table, except for the cases where we ablate certain parameters. The only hyperparameters that change across benchmarks are the number of steps for the learning rate warmup and the number of input frames. The number of warmup steps depends on the dataset size and corresponds to 10% of the total number of steps, i.e.

$$\#steps_{warmup} = 0.1 * \#steps/epoch * \#epochs \quad (2)$$

**Table 6:** Ablation on the number of trainable parameters.

LoRA Rank (# trainable parameters)	R1@0.5	R1@0.7	mIoU
2 (6M)	66.03	43.03	56.59
4 (10M)	65.71	43.59	56.78
8 (19M)	67.28	<b>46.70</b>	<b>57.46</b>
16 (37M)	<b>67.72</b>	45.38	57.35

**A girl is excited about showing her bed with a big red heart in it.**

**Fig. 4:** We observe the capability of our model to recognize and differentiate 3 separate moments that repeatedly occur with intermittent interruptions. Each predicted moment depicts the respective natural language query.

## B Additional Results

### B.1 Effect of number of trainable parameters

In the main paper, we state the use of parameter-efficient finetuning techniques and thus training only a small number of parameters. In practice, we leverage LoRA [22] with a rank set to 8 and apply it to all linear layers in the large language model, yielding about 19 million trainable parameters.

In Table 6, we show the effect of different LoRA ranks and their resulting number of trainable parameters. We observe that setting the rank to 16, i.e. training double the number of parameters does not yield any significant improvement (row 4). Moreover, training fewer parameters, i.e. 10 or 6 million, by setting the rank to 4 or 2, respectively, does degrade the performance of *Mr. BLIP* (rows 1 and 2).

## C Additional Qualitative Results

In this section, we provide further qualitative results and discuss shortcomings of our model that can be addressed in future research. For each example, we provide the discussion in the respective caption for the convenience of the reader. Examples 1 through 6 are from QVHighlights [33] and examples 6 through 10 are from Charades-STA [20].

As in the main paper, we illustrate the ground truth targets as dashed lines and the predicted windows as solid lines.

**Donald Trump speaks in large circular table.****Fig. 5:** *Mr. BLIP* can recognize a distinct public figure, Donald Trump, although the training set includes only 6 queries containing Donald Trump.**Man and woman sit on opposite sides of circle desk.****Fig. 6:** Our model predicts a third window, that does not align with a ground truth moment, which, in fact, is accurate and depicts the query.**A mom holds on to her child in the snow.****Fig. 7:** *Mr. BLIP* accurately predicts 3 out of 4 moments. It fails to predict the first moment, which lasts for only 2 seconds. This is likely because we sample a frame every 2.5 seconds and, by chance, might not sample one in the respective window.**Soldiers escort people through the wilderness.****Fig. 8:** The video contains two groups of relevant moments which contain a short sub-2-second cut that does not depict the query. With a resolution of 60 frames for a 150-second long video, corresponding to a frame being seen every 2.5 seconds, *Mr. BLIP* can not detect the cut and predicts two long moments that encompass the two short ones. Moreover, our model predicts a third window (red) that does not match a ground truth label. The predicted moment does in actuality depict soldiers, but those are not escorting other people.**A herd of bison is shown crossing the road.****Fig. 9:** Our model has trouble predicting very short moments in long videos and high-frequency jump cuts given the resolution of the frame sampling.

**a person awakens in a bedroom.**



**Fig. 10:** Given a very ambiguous query, our model’s prediction aligns with the ground truth.

**a person closes a front door.**



**Fig. 11:** Our model fails to recognize the action of the man closing the front door. We hypothesize this is because the door is very dark and poorly visible. Our model predicts the moment when the door is clearly visible and closed.

**the person puts the broom down.**



**Fig. 12:** Our model fails to recognize the action of putting down the broom at the beginning of the video and predicts the moment when the man picks the broom back up and then holds it.

**the person begins sneezing.**



**Fig. 13:** *Mr. BLIP* recognizes the moment when the person is sneezing. The ground truth is false.